Structural and magnetic properties of $Mg_xSr_xMn_xCo_{1-3x}Fe_2O_4$ nanoparticle ferrites

Nadir SE. Osman, Thomas Moyo and Hafiz M I Abdallah

School of Chemistry and Physics, University of KwaZulu-Natal, Westville campus, P/Bag X5400, Durban 4000, South Africa

Osmann@ukzn.ac.za

Abstract: A series of $Mg_xSr_xMn_xCo_{1-3x}Fe_2O_4$ nanoferrites (with x =0, 0.1, 0.2, 0.3, 1/3) were synthesized by glycol-thermal technique. X-ray diffraction (XRD) patterns of the as-prepared samples show single-phase cubic spinel structure. The average crystallite sizes, lattice parameters, XRD densities and porosities were estimated from XRD data. The average crystallite sizes were found in range of 7.5 to 9 nm. Mössbauer spectroscopy measurements were performed in order to investigate the magnetic order of the materials and the distribution of Fe^{3+} ions in the tetrahedral and octahedral sites. Room temperature magnetic measurements of the series were studied using a vibrating sample magnetometer. The results show that the values of the coercive fields and saturation magnetizations which increase with increase in Co content from 15 Oe and 56.51 emu/g for x=0.3 to 114 Oe and 76.61 emu/g for x= 0.1 respectively. Significant correlations between magnetizations and coercive fields are observed. A significant change in properties is observed for the $Mg_xSr_xMn_xCo_{1-3x}Fe_2O_4$ compound. These results are contrasted with low temperature measurements from 2 K to 300 K and magnetic fields to 5 Tesla.

Keywords: *Glycol-thermal, Nanoferrite; Spin-freezing; superparamagnetism, exchange-interaction*

1. Introduction

Nanoparticles have special magnetic and electrical properties that are significantly different from their corresponding bulk materials [1, 2]. Reduction in the scale of the bulk materials to less than 100 nm can produce materials that exhibit exceptional properties such as superparamagnetic relaxation phenomena and spin-canted structure due to surface effects [3]. Magnetic nanoparticles have been attracting considerable interest because of a variety of possible applications [4-5]. Therefore understanding the magnetic properties of nanoscale particles is a central issue in magnetic materials. Ferrites and related compounds have been found to be suitable for many applications such as making cores for audio frequency, high frequency transformers, coils, chokes, permanent magnets, magneto-optical displays, microwave absorbers and guides in gas sensors [6-7]. Spinel nanoferrites are amongst materials with interesting optical, magnetic and electrical properties [8]. By changing the divalent elements in the tetrahedral sites of the spinel, the magnetic properties can be tuned. $CoFe_2O_4$ ferrite is known for its good magnetostriction properties, magneto-crystalline anisotropy and moderate saturation magnetization. These features make $CoFe_2O_4$ an interesting system study. Abdallah *et al* [9]

reported enhanced magnetic properties of a sample $Mn_{0.3}Co_{0.7}Fe_2O_4$ by Mg and Sr substitutions. The results showed significant changes in the magnetic properties compared to the initial parent material. Jigajeni *et al* [10] have also reported that $Mn_{0.2}Mg_{0.3}Co_{0.7}Fe_{1.8}O_4$ is a good candidate for magnetoelectric applications because of favorable values of resistivity, saturation magnetization and coercive field. We have therefore extended these studies by performing simultaneous substitutions of Co by Mg, Sr and Mn in $CoFe_2O_4$ for a series of samples with equal atomic proportions of substituting elements. The intention is to investigate any structural and magnetic changes due to the symmetry in the stoichiometry of the substituting elements.

2. Experimental details

$Mg_xSr_xMn_xCo_{1-3x}Fe_2O_4$ (x = 0, 0.1, 0.2, 0.3, 0.33) nanoferrites were synthesized by the glycol-thermal method in a Watlow series model PARR 4843 stirred pressure reactor. The starting materials were high purity $CoCl_2.6H_2O$, $Fe_2Cl_3.6H_2O$, $MnCl_2.4H_2O$, $MgCl_2.6H_2O$ and $SrCl_2.6H_2O$. Full details of the synthesis method used in the present case have been reported elsewhere [11]. The phase and structural characterization of the samples were obtained by a Phillips X-ray diffractometer (XRD) type PW1710 using CoKα radiation. The average crystallite size was calculated from the most intense (311) XRD peak. The morphology of nanoparticle was investigated by high-resolution transmission electron microscopy (HRTEM) (type: Jeol_JEM-1010). The microstructures of samples were investigated by high-resolution scanning electron microscope (HRSEM). ^{57}Fe Mössbauer spectra were obtained by a conventional spectrometer using a ^{57}Co source sealed in Rh matrix and vibrated at constant acceleration. Magnetic measurements were performed at room temperature using a LakeShore model 735 vibrating sample magnetometer (VSM). A mini cryogen free measurement system was used to perform low temperature magnetization measurements from 2 to 300 K.

3. Results and discussion

Figure 1 shows the X-ray diffraction patterns of the as-prepared samples of $Mg_xSr_xMn_xCo_{1-3x}Fe_2O_4$ series. The patterns indicate that single phase spinel structures were formed and no impurity peaks were observed. All the patterns are in match with the standard patterns of spinel ferrite. The average grain sizes were calculated using the Scherrer equation $D = 0.9\lambda/(\beta\cos\theta)$, where β is the full-width at half-maximum of the most intense (311) XRD peak [12].

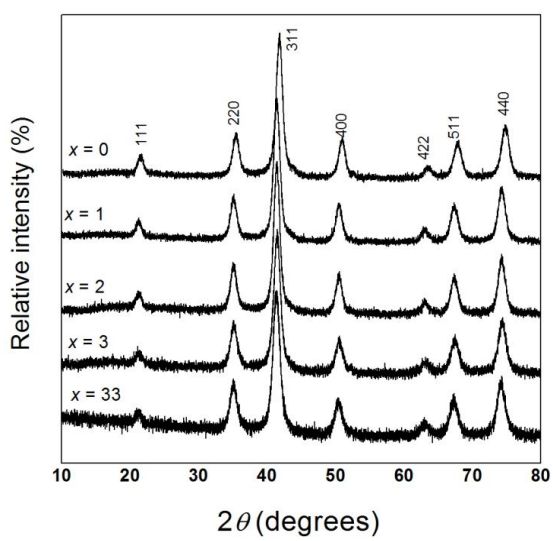

Fig. 1. X-ray patterns for the as-prepared samples of $Mg_xSr_xMn_xCo1\text{-}3_xFe_2O_4$ nanoparticle ferrites.

The lattice parameter a, was calculated using Bragg's law and equation $a = d(h^2+k^2+l^2)^{1/2}$ where d is the inter-planar spacing [13]. The XRD densities ρ_{XRD} were calculated using the formula $\rho_{XRD} = 8M_0 / N_A a^3$ where M_o is the molecular weight and N_A is the Avogadro's number. The calculated lattice parameters a, crystallite sizes D, X-ray densities ρ_{XRD}, are presented in Table 1.The lattice parameter of the sample for x = 0 was found to be similar to a reported value [14]. However, there is no significant changes in the lattice parameters after substitution of Co except for the sample at x = 0.33 which shows a relatively high lattice parameter value. The XRD density values are observed to decrease with decreasing Co content.

The microstructure and the surface morphology were studied by means of HRTEM and HRSEM respectively. Figure 2 shows typical HRTEM micrographs showing uniform and nearly spherical nanoparticles with some agglomeration. Agglomeration can enhance the magnetic interaction between the nanoparticles [15]. The boundaries between the crystallites can also be clearly observed. The values of the crystallite sizes estimated from the images are also given in table 1 and appear to be consistent with the estimates from the XRD data. Figure 3 shows the HRSEM surface morphology of the as-prepared $Mg_xSr_xMn_xCo_{1-3x}Fe_2O_4$ which also support the observation from HRTEM.
Figure 4 shows room-temperature Mössbauer spectra for the as-prepared $Mg_xSr_xMn_xCo_{1-3x}Fe_2O_4$ samples at 300 K. Two sextets were used to fit the Mössbauer data and an additional one was required for the sample at $x = 0.1$ in order to obtain a better fit to the data. This additional sextet is attributed to the presence of Fe^{3+} in the grain boundaries [17].

Table 1: The lattice parameters (a), crystallite sizes (D), X-ray densities (ρ_{XRD}) of the series $Mg_xSr_xMn_xCo_{1-3x}Fe_2O_4$.

x	a (Å) ±0.003	D_{XRD} (nm) ±0.01	D_{HRTEM} (nm) ±1.69	ρ_{XRD} (g/cm^3) ±0.001
0.0	8.380	8.27	8.55	5.296
0.1	8.387	7.91	8.33	5.261
0.2	8.387	8.34	8.66	5.237
0.3	8.379	7.28	7.42	5.230
0.33	8.395	7.20	7.83	5.182

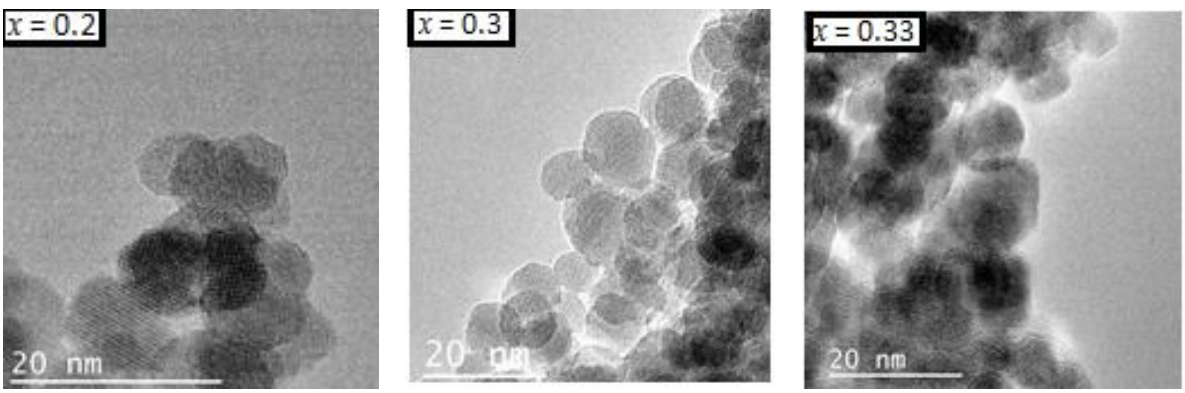

Figure 2. HRTEM images for the as-prepared $Mg_xSr_xMn_xCo_{1-3x}Fe_2O_4$samples.

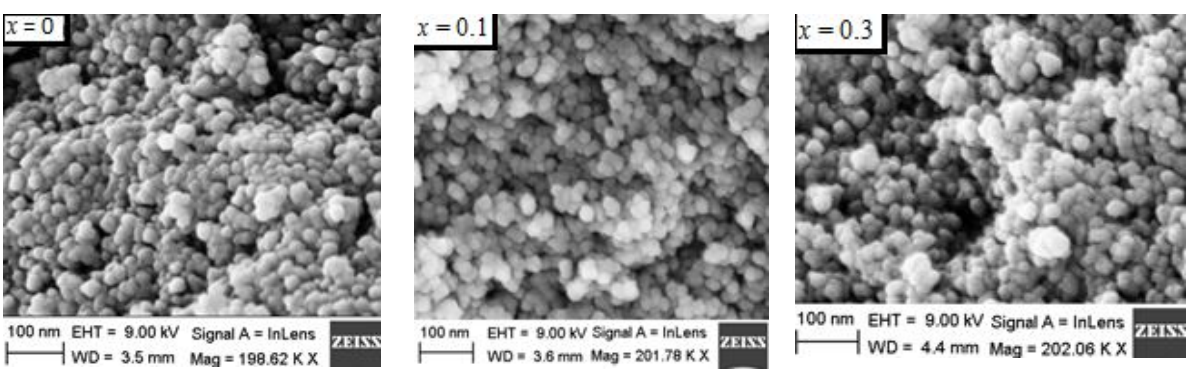

Figure 3. HRSEM micrographs for the as-prepared $Mg_xSr_xMn_xCo_{1-3x}Fe_2O_4$ samples.

The results of the hyperfine parameters are presented in table 2. Larger values of hyperfine fields are assigned to the B-sites [9, 17]. A decrease in hyperfine fields is observed which is associated with the reduction of Co content in the samples for $x > 0.1$. The isomer shift values are associated with Fe^{3+} ions [18] and show no significant changes with composition.

Figure 5 shows the hysteresis loops of the as-prepared $Mg_xSr_xMn_xCo_{1-3x}Fe_2O_4$ measured at an applied field of about 14 kOe at 300 K. Slightly substituting Co by Mg, Sr and Mn atoms significantly increases the value of the magnetization from 32.79 emu/g to 76.61 emu/g for x=0.1. There after the magnetization decreases with increasing x to 32.87 emu/g when x = 0.33. However, more reliable trends in coercive fields and magnetization need to be deduced for $H >> 14$ kOe. Room temperature magnetic properties can be understood in term of cations distribution [8] based on superexchange interaction between A and B sites. The increases in the saturation magnetization can be attributed to the magnetic moments of 5 μ_B Mg or Mn with the addition of Mn favoring more negative exchange interactions. The result show the coercivity decreases proportionally with the increase in x reflecting the decline in the Co atoms which are associated with high uniaxial anisotropy [19]. Table 3 also shows magnetic parameters deduced from magnetization measurements at room temperature. The magnetic moments can be deduced from saturation magnetizations [20].

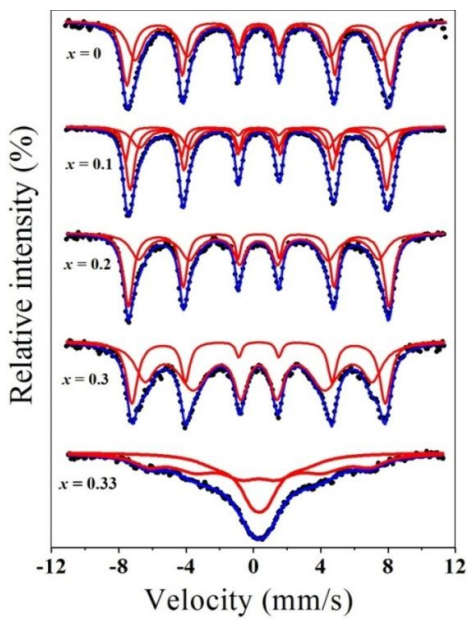

Figure 4. Mössbauer spectra for the as-prepared $Mg_xSr_xMn_xCo_{1-3x}Fe_2O_4$ samples at 300 K.

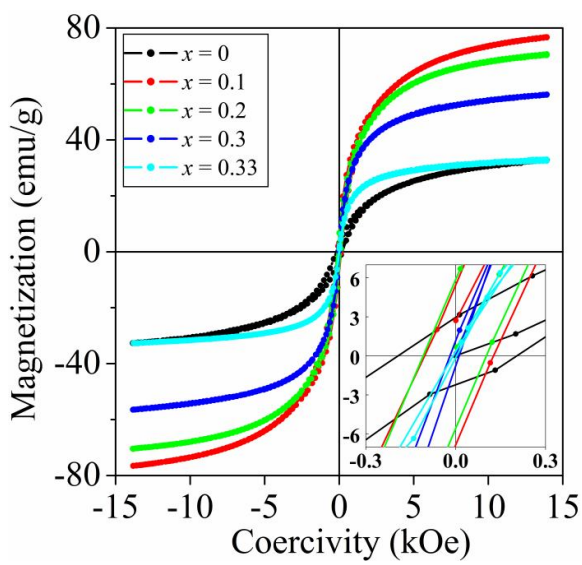

Figure 5. Room temperature hysteresis loop of $Mg_xSr_xMn_xCo_{1-3x}Fe_2O_4$ as-prepared. The inset shows magnified view of $M - H$ curves.

Table 2. Isomer shifts (δ), hyperfine magnetic fields (H), line widths (Γ) and Fe^{3+} fraction population (f) on A- and B- sites for the as-obtained $Mg_xSr_xMn_xCo_{1-3x}Fe_2O_4$ samples.

x	δ (mm/s)		H (kOe)			Γ (mm/s)		f (%)	
	δ_A ±0.03	δ_B ±0.04	H_A ±9	H_B ±4	H_{3rd} ±7	Γ_A ±0.09	Γ_B ±0.08	f_A ±3	f_B ±7
0	0.31	0.31	453	485	-	0.32	0.24	50	50
0.1	0.30	0.34	473	493	439	0.26	0.21	41	24
0.2	0.31	0.31	442	480	-	0.42	0.17	49	51
0.3	0.32	0.32	419	467	-	0.55	0.21	70	30
0.33	0.38	0.34	161	409	-	0.94	1.35	47	53

The values of M_R/M_S indicate the hysteresis loop squareness [15], which can be a guide to how the nanoparticles could be used in different applications. It is also observed that the highest squareness value is observed when $x = 0.2$.

Low temperature magnetic measurements at a maximum applied field of 50 kOe were performed which can provide more reliable trends in the current series of compounds. *M - H* curves in figure 6 reveal some distortion of the hysteresis loops at 2 K for the samples at $x = 0.1$ and $x = 0.2$. We suggest this distortion to be due to the decoupling between the hard and soft magnetic phases. Upadhyay *et al* [21] have explained similar hysteresis loop behavior in terms of freezing of disordered spins. No distortions of the loops are observed for the samples at $x = 0$, 0.3, 0.33. The magnetization does not saturate even in fields of 50 kOe. Figure 7 shows the variation of the coercivity and the magnetization with the temperature. Both parameters are sensitive to temperature change and the effect of spin freezing [9]. Significant increases in coercive fields with temperature are observed for samples with $x = 0.1$, 0.2 and 0.3. The highest coercive field is obtained for $x = 0.1$ and the least for $x = 0.3$. The samples corresponding to $x = 0$ and 0.33 do not show significant changes in coercive fields at low temperatures.

Table 3. Magnetic parameters of $Mg_xSr_xMn_xCo_{1-3x}Fe_2O_4$ measured at 300 K.

x	H_c (Oe)	M_S (emu/g)	M_R (emu/g)	M_R/M_S	n_B (μ_B)
0.0	198.15	32.79	2.59	0.078	2.37
0.1	114.92	76.61	6.14	0.077	3.18
0.2	105.61	70.56	5.73	0.081	2.94
0.3	15.34	56.51	0.97	0.017	2.34
0.33	5.89	32.87	0.24	0.007	1.36

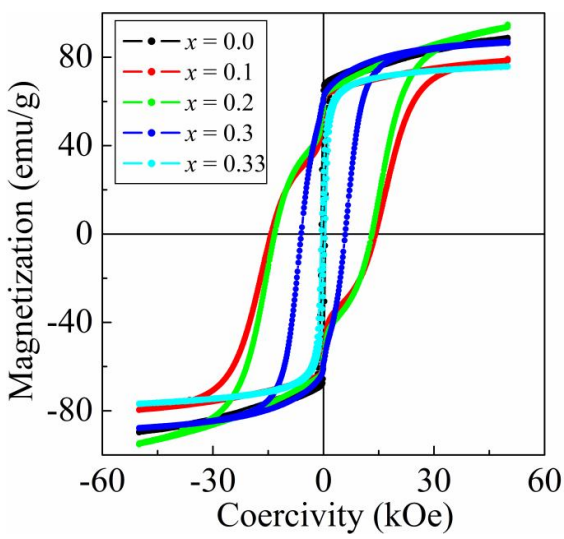

Figure 6. *H – M* loops for $Mg_xSr_xMn_xCo_{1-3x}Fe_2O_4$ as-prepared measured at 2 K.

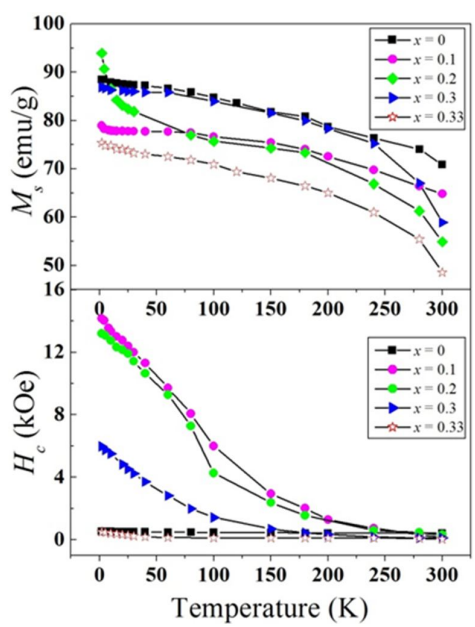

Figure 7. Variations of coercivity and saturation magnetization as function of measuring temperature for the as-prepared samples of $Mg_xSr_xMn_xCo_{1-3x}Fe_2O_4$.

4. Conclusions

$Mg_xSr_xMn_xCo_{1-3x}Fe_2O_4$ series have been successfully synthesized using glycol-thermal technique. XRD patterns indicated the formation of single phase spinel crystallites which are nearly spherical in shaped with sizes from about 7.5 to 8.5 nm. Hence simultaneous substitution of Co by Mg, Mn and Sr was achieved. Low temperature measurements show interesting trends in the magnetization and coercive fields. The samples with the highest and least Co content (x =0 and x = 0.33) show the least sensitivity to changes in coercive fields and magnetization at low temperatures. Significant enhancement of the coercive fields are obtained for $0.1 \leq x \leq 0.3$.

Acknowledgments

The authors would like to thank the National Research Foundation (NRF) of South Africa for equipment grants and Sudan University of Science and Technology for the study leave (NSEO).

References

[1] Pankhurst A, Connolly J, Jones S K, Dobson J 2003 *J. Phys. D: Appl. Phys.* **36** R167
[2] Kodama R H 1999 *J. Magn. Magn. Mater.* 359
[3] Didukh P, Greneche J M, lawska-Waniewska A S, Fannin P C, Casas L 2002 *J. Magn. Magn. Mater.* **242** 61
[4] Mornet S, Vasseir S, Grasset F, Duguet E 2004 *J. Mater. Chem.* **14** 216
[5] Lin X M, Samia A C S 2006 *J. Magn. Magn. Mater.* **305** 100
[6] Blasse G 1964 *Philips Research Reports Suppl.* **3** 96
[7] Nejati K, Zabihi R 2012 *Chem. Cent. J.* **6** 23
[8] Ashiq M, Saleem S, Malana M, Ur-Rehman A 2009 *J. AlloysComp.* **486** 640
[9] Abdallah H M I, Moyo T 2013 *J. Alloys Comp.* **562** 156
[10] Jigajeni S, Kulkarni S R, Kolekar Y, Kulkarni S B, Joshi P 2010 *J. Alloys Comp.* **402** 492
[11] Abdallah H.M.I, Moyo T, Msomi J.Z 2011 *J Supercond Nov Magn* **24** 673.
[12] Naseri M G, Saion E B, Ahangar H A, Hashim M, Shaari A H 2011 *J. Magn. Magn. Mater.* **323** 1745
[13] Kittel C 2005 *Introduction to Solid State Physics*, 5th edition, John Wiley & Sons pp. 302–304
[14] Dascalu G, Popescu T, Feder M, Caltun O F 2013 *J Magn. Magn. Mater.* **333** 69
[15] Aslibeiki B, Kameli P, Salamati H, Eshraghi M, Tahmasebi T 2010 *J. Magn. Magn. Mater.* **322** 2929
[16] Maaz K, Mumtaz A, Hasanain S K, Ceylan A 2007 *J. Magn. Magn. Mater.* **308** 289
[17] Manova E, Kunev B, Paneva D, Mitov I, Petrov L, Estournes C, D'Orleans C, Rehspringer J, Kurmoo M 2004 *Chem. Mater.* **16** 5689
[18] Jing J, Zhao F, Yang X, Gonser U 1990 *Hyperfine Interaction* **54** 571
[19] Chakrabarti S, Mandal S K, Chaudhuri S 2005 *Nanotechnology***16** 506
[20] Kambale R C, Shaikh P A, Kamble S S, Kolekar Y D 2009 *J. Alloys Comp.* **478** 599
[21] Papaefthymiou G C, Ahmed S R, Kofinas S 2005 *Rev. Adv. Mater. Sci.* **10** 306